Indian Journal of Chemistry
Vol. 63, February 2024, pp. 145-158
DOI: 10.56042/ijc.v63i2.4273

# Design, synthesis, *in vitro* and computational analyses of anticancer nicotinamide derivatives

Muhammed Gömeç[a], Vesim Nasif[b], Ayşe Hümeyra Taşkin Kafa[c], Koray Sayin[b]*, Hayreddin Gezegen[d] & Hilmi Ataseven[e]

[a] Department of General Surgery, Faculty of Medicine, Cumhuriyet University, Sivas, Türkiye

[b] Department of Chemistry, Faculty of Science, Sivas Cumhuriyet University, Sivas, Türkiye

[c] Department of Medical Microbiology, Faculty of Medicine, Cumhuriyet University, Sivas, Türkiye

[d] Department of Nutrition and Dietetics, Faculty of Health Sciences, Cumhuriyet University, Sivas, Türkiye

[e] Department of Gastroenterology, Faculty of Medicine, Sivas Cumhuriyet University, Sivas, Türkiye

E-mail: krysayin@gmail.com

*Received 22 July 2023; accepted (revised) 19 January 2024*

The search for ideal treatment continues for many health problems such as cancer and infection. In this context, new synthesis compounds have been promising and the nicotinamide derivative compounds, which is an important heterocyclic derivative, has attracted the attention of many researchers. Nowdays, anticancer, antifungal, antimicrobial, antibacterial and antibiofilm effects of some nicotinamide derivatives have been demonstrated. In this study, nine new nicotinamide derivative compounds have been designed and synthesized. The characterization of these synthesized compounds have been done by *in silico* methods. The anticancer effects of the compounds have been investigated in four different cancer types and compared with their effects on healthy fibroblast cells. N4 has been found to have a cytotoxic effect on MCF-7 human breast cancer, and the IC50 value has been calculated as 12.1 µM. In addition, antibacterial, antifungal and antibiofilm activities were investigated by *in vitro* methods and they have been shown to be effective. As a result, it is observed that N4, one of the newly synthesized nicotinamide derivative compounds, has a serious cytotoxic effect in MCF-7 human breast cancer cells compared to healthy fibroblast cells. Pharmacophore map and ADME analyses of studied compound are performed in detail.

**Keywords**: Nicotinamide, Synthesis, DFT, *In silico*, Anticancer

Nicotinamide and its derivatives are a significant class of heterocyclic derivatives[1]. These compounds have attracted the attention of many researchers and have been shown to have a broad application range until today[1-12]. Considering the application area of the compounds, it is seen that they are frequently tried especially in health and agriculture. Some properties which are antifungal, antimicrobial, antibacterial, antibiofilm have been explored. Additionally, nicotinamide class compounds have anti-dandruff, anti-itching, hair growth-promoting, grey hair preventing properties and they increase hair elasticity and treat acne, fine lines as well as age spots. Especially, nicotinamide has anticancer properties. Especially, these compounds are reported as tyrosine kinase (TKI) and histonedeacetylase (HDAC) inhibitors. For instance, N-(4-(1-cyanocyclopentyl) phenyl)-2-((pyridin-4-ylmethyl)amino)nicotinamide (A) known as "apatinib" and N-(4-(2-(4-methylbenzylidene) hydrazine-1-carbonyl)phenyl) nicotinamide (B), which are represented in Fig. 1, are TKI and HDAC inhibitors, respectively[13].

In this study, nine nicotinamide derivatives which are represented in Scheme 1 are focused. These compounds are initally synthesized and characterized using spectral techniques (IR, $^{1}$H-NMR, $^{13}$C-NMR and LC-QTOF-MS). Then, they are fully-optimized at B3LYP/6-31+G(d) level in water with the C-PCM solvent method. Electronic properties of these compounds are examined using contour plots of frontier molecular orbital and molecular electrostatic potential (MEP) map of them.

Furthermore, biological activity which are anticancer, antibacterial and antibiofilm are investigated in detail. For this aim, anticancer properties of these compounds are examined against breast cancer (MCF-7), colon cancer (HT-29) and gastric cancer (SNU-1 and SNU-16). The best candidate is found as **N4**. Antibacterial and antifungal activity of studied compounds are investigated against *Staphylococcus aureus* (ATCC 29213), Methicillin-

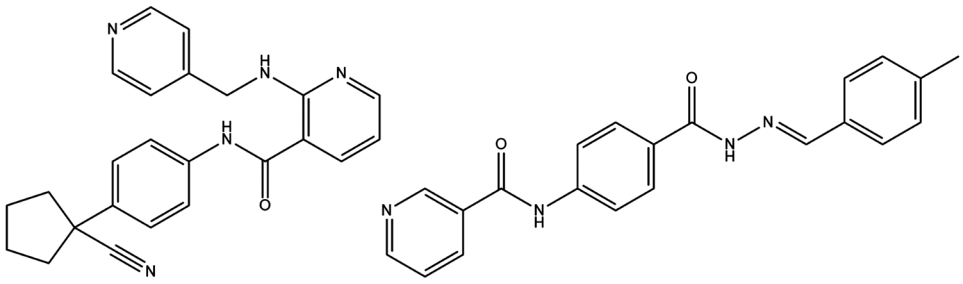

Fig. 1 — Structure of nicotinamide derivative

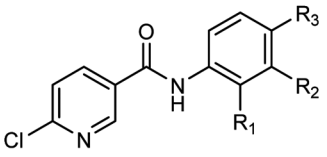

| Assignment | $R_1$ | $R_2$ | $R_3$ |
|---|---|---|---|
| N1 | H | H | H |
| N2 | Cl | H | $CF_3$ |
| N3 | H | $CF_3$ | Cl |
| N4 | H | H | $CF_3$ |
| N6 | H | H | $SCH_3$ |
| N7 | H | $SCH_3$ | H |
| N8 | Cl | H | H |
| N9 | H | Cl | H |

Scheme 1 — Schematic structure of studied compounds

resistant *S. aureus* (ATCC 43300), *Enterococcus faecalis* (ATCC 29212), *Escherichia coli* (ATCC 25922), *Pseudomonas aeruginosa* (ATCC 27853), *Klebsiella pneumoniae* (ATCC 700603), *Candida albicans* (ATCC10231). **N2 and N3** exhibit the best antibacterial activity.

## Experimental Section

### Reagents

6-chloronicotinoyl chloride, 2-chloroaniline, 3-chloroaniline, 4-chloroaniline, 2-bromoaniline, triethylamine and solvents which are dichloromethane (DCM), 1,2-dichloroethane (1,2-DCE), chloroform, petroleum ether, diethyl ether, DMSO was purchased from Merck kGaA.

### Instrumentation

IR spectra (4000–400 $cm^{-1}$) were obtained using IR spectra (ATR) and recorded on a Bruker Tensor II FT-IR spectrometer. Melting points were measured on an Electrothermal IA9100 apparatus. $^1$H-NMR and $^{13}$C-NMR spectra were recorded on a JEOL (400MHz) JNM-ECZ400S/L1 NMR instrument in DMSO-$d_6$ at room temperature; δ in ppm relative to tetramethylsilane (TMS), with J in hertz (Hz). Agilent Technology Inc. of 1260 Infinity HPLC System was coupled with 6530 Q-TOF LC/MS detector and ZORBAX SB-C18 (2.1×50mm, 1.8 μm) column. $^1$H-NMR, $^{13}$C-NMR, and Q-TOF LC/MS analyses of the compounds were carried out at the Advanced Technology Application and Research Center (CUTAM) of Sivas Cumhuriyet University.

### Synthesis of nicotinamide derivatives

Related nicotinamide derivatives were synthesized according to Fig. 2. Related aniline derivatives are added to the solution of 6-chloronicotinoyl chloride in DCM:1,2-DCE (1:1) with trimethylamine. The mixture were refluxed nearly 3h and extracted with $CH_2Cl_2$ three times. The organic part was dried $Na_2SO_4$ and evaporated. The residue was crystallized in ethanol/$CHCl_3$ (8:2). This synthesis route has been used by Sayin et al. 2022[14].

The synthesized compounds were characterized by spectral characterization techniques, IR, $^1$H NMR, $^{13}$C NMR, and LC-QTOF-MS. The related spectrum

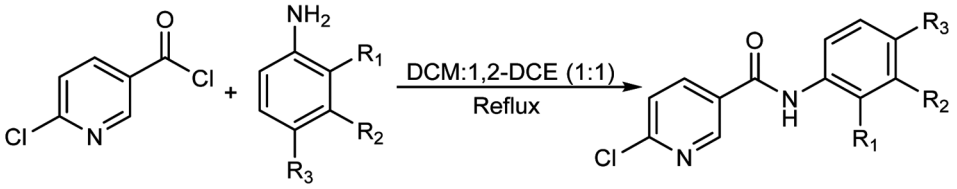


Fig. 2 — Synthesis scheme

are given in Supp. Material. The obtained results are given as follows for each compound.

**2-Chloro-N-(2-chlorophenyl)nicotinamide** (**N1**): Yield: 63%. White crystal. IR ($cm^{-1}$): 3307, 3138, 3045, 2117, 2085, 1990, 1874, 1647, 1605, 1579, 1532, 1495, 1436, 1366, 1327, 1268, 1247, 1184, 1140, 1100, 1077, 1017, 939, 905, 884, 844, 735, 683, 657, 590, 536, 500, 477, 410. $^{1}$H NMR (400 MHz, DMSO-$D_6$) δ 10.44, 8.89 (d, $J$ = 2.5 Hz, 1H), 8.29 (dd, $J$ = 8.3, 2.5 Hz, 1H), 7.70 (d, $J$ = 8.1 Hz, 2H), 7.65 (dd, $J$ = 8.3, 0.7 Hz, 1H), 7.34 – 7.29 (m, 2H), 7.10 – 7.05 (m, 1H). $^{13}$C NMR (101 MHz, DMSO-$D_6$) δ 163.42, 153.27, 149.85, 139.60, 139.16, 130.49, 129.26 (2C), 124.66 (2C), 120.88 (2C). HPLC-TOF/MS: 231.0335 ([M-H]$^-$, $C_{12}H_9ClN_2O^-$; calc. 231.0331).

**2-Chloro-N-(2-chlorophenyl)nicotinamide** (**N2**): Yield: 68%. Off-white crystal. IR ($cm^{-1}$): 3319, 3078, 1667, 1586, 1526, 1458, 1398, 1314, 1271, 1244, 1172, 1108, 1078, 1021, 890, 842, 755, 703, 643, 610, 544, 450. $^{1}$H NMR (400 MHz, DMSO-$D_6$) δ 10.55, 8.92 (dd, $J$ = 2.5, 0.6 Hz, 1H), 8.31 (dd, $J$ = 8.3, 2.6 Hz, 1H), 7.93 (d, $J$ = 1.6 Hz, 1H), 7.86, 7.84, 7.73 (dd, $J$ = 2.1, 0.8 Hz, 1H), 7.67 (dd, $J$ = 8.3, 0.7 Hz, 1H). $^{13}$C NMR (101 MHz, DMSO-$D_6$) δ 163.78, 153.86, 150.03, 139.73, 138.93, 129.89, 129.24, 128.85, 128.15 (q, $J$ = 32.8 Hz), 127.88, 127.30 (d, $J$ = 3.6 Hz), 127.25, 125.13 (d, $J$ = 3.6 Hz), 124.82, 122.46. HPLC-TOF/MS: 332.9821 ([M-H]$^-$, $C_{13}H_7Cl_2F_3N_2O^-$; calc. 332.9815).

**2-Chloro-N-(2-chlorophenyl)nicotinamide** (**N3**): Yield: 71%. Cream crystal. IR ($cm^{-1}$): 3334, 3131, 3079, 1686, 1592, 1535, 1477, 1412, 1320, 1251, 1104, 1027, 898, 826, 754, 663, 533, 450. $^{1}$H NMR (400 MHz, DMSO-$D_6$) δ 10.77, 8.89 (d, $J$ = 2.5 Hz, 1H), 8.29 (dd, $J$ = 8.4, 2.5 Hz, 1H), 8.25 (d, $J$ = 2.5 Hz, 1H), 8.00 (dd, $J$ = 8.8, 2.6 Hz, 1H), 7.66 (dd, $J$ = 8.6, 4.0 Hz, 1H). $^{13}$C NMR (101 MHz, DMSO-$D_6$) δ 163.87, 153.72, 149.93, 139.60, 138.68, 132.65, 129.78, 127.22 (q, $J$ = 30.8 Hz), 125.49, 125.31, 124.77, 124.58, 121.86, 119.47 (q, $J$ = 5.6 Hz), 119.14, 40.62, 40.41, 40.20, 39.99, 39.78, 39.57, 39.36. HPLC-TOF/MS: 332.981 ([M-H]$^-$, $C_{13}H_7Cl_2F_3N_2O^-$; calc. 332.9815).

**2-Chloro-N-(2-chlorophenyl)nicotinamide** (**N4**): Yield: 51%. Cream crystal. IR ($cm^{-1}$): 3314, 3056, 1653, 1584, 1522, 1462, 1407, 1319, 1249, 1160, 1106, 1063, 1017, 905, 833, 761, 654, 409. $^{1}$H NMR (400 MHz, DMSO-$D_6$) δ 10.74, 8.91 – 8.90 (m, 1H), 8.30 (dd, $J$ = 8.3, 2.5 Hz, 1H), 7.94, 7.91, 7.68, 7.67 – 7.66 (m, 1H), 7.64. $^{13}$C NMR (101 MHz, DMSO-$D_6$) δ 163.96, 153.59, 149.97, 142.80, 139.70, 130.08, 126.53 (d, $J$ = 3.7 Hz), 120.71, 40.61, 40.40, 40.19, 39.98, 39.77, 39.56, 39.36. HPLC-TOF/MS: 299.0204 ([M-H]$^-$, $C_{13}H_8ClF_3N_2O^-$; calc. 299.0204).

**2-Chloro-N-(2-chlorophenyl)nicotinamide** (**N5**): Yield: 79%. Yellow crystal. IR ($cm^{-1}$): 3271, 3043, 1644, 1583, 1526, 1492, 1457, 1394, 1329, 1145, 1105, 1016, 903, 807, 671, 503, 409. $^{1}$H NMR (400 MHz, DMSO-$D_6$) δ 10.43, 8.88 (dd, $J$ = 2.6, 0.8 Hz, 1H), 8.28 (dd, $J$ = 8.3, 2.5 Hz, 1H), 7.70 – 7.61 (m, 1H), 7.25 – 7.20 (m, 1H). $^{13}$C NMR (101 MHz, DMSO-$D_6$) δ 163.26, 153.28, 149.82, 139.54, 136.52, 133.53, 130.39, 127.25, 124.65, 121.53, 15.78. HPLC-TOF/MS: 277.0208 ([M-H]$^-$, $C_{13}H_{11}ClN_2OS^-$; calc. 277.0208).

**2-Chloro-N-(2-chlorophenyl)nicotinamide** (**N6**): Yield: 64%. Dark green crystal. IR ($cm^{-1}$): 3304, 3065, 2117, 1863, 1667, 1595, 1585, 1538, 1469, 1394, 1366, 1327, 1294, 1241, 1101, 968, 851, 778, 757, 682, 637, 531, 409. $^{1}$H NMR (400 MHz, DMSO-$D_6$) δ 10.43, 8.89 (d, $J$ = 2.5 Hz, 1H), 8.29 (dd, $J$ = 8.3, 2.5 Hz, 1H), 7.69 – 7.62 (m, 2H), 7.53 – 7.46 (m, 1H), 7.25 (t, $J$ = 8.0 Hz, 1H), 6.97 (ddd, $J$ = 7.9, 1.9, 0.9 Hz, 1H), 2.42. $^{13}$C NMR (101 MHz, DMSO-$D_6$) δ 163.51, 153.37, 149.85, 139.73, 139.58, 139.17, 130.36, 129.77, 124.68, 121.94, 117.81, 117.27, 15.11. HPLC-TOF/MS: 277.0204 ([M-H]$^-$, $C_{13}H_{11}ClN_2OS^-$; calc. 277.0208).

**2-Chloro-N-(2-chlorophenyl)nicotinamide** (**N7**): Yield: 54%. Cream crystal crystal. IR ($cm^{-1}$): 3280, 3060, 2116, 1903, 1642, 1585, 1528, 1469, 1435, 1365, 1312, 1269, 1137, 1098, 1053, 1015, 901, 838, 737, 631, 535. $^{1}$H NMR (400 MHz, DMSO-$D_6$) δ 10.35, 8.93 – 8.92 (m, 1H), 8.32 (dd, $J$ = 8.3, 2.5 Hz, 1H), 7.67 (dd, $J$ = 8.3, 0.6 Hz, 1H), 7.53 (td, $J$ = 8.0, 1.5 Hz, 1H), 7.35 (td, $J$ = 7.7, 1.5 Hz, 1H), 7.27 (td, $J$

= 7.7, 1.7 Hz, 1H). $^{13}$C NMR (101 MHz, DMSO-$D_6$) δ 163.57, 153.63, 149.88, 139.59, 134.95, 130.20, 130.13, 129.54, 129.14, 128.48, 128.12, 124.84. HPLC-TOF/MS: 264.9937 ([M-H]$^-$, $C_{12}H_8Cl_2N_2O^-$; calc. 264.9941).

**2-Chloro-N-(2-chlorophenyl)nicotinamide** (**N8**): Yield: 57%. Cream crystal. IR (cm$^{-1}$): 3281, 3069, 2108, 1863, 1647, 1580, 1540, 1462, 1400, 1324, 1099, 1018, 875, 795, 731, 675, 535, 415. $^1$H NMR (400 MHz, DMSO-$D_6$) δ 10.58, 8.89 – 8.88 (m, 1H), 8.29 (dd, *J* = 8.3, 2.5 Hz, 1H), 7.88 (t, *J* = 2.0 Hz, 1H), 7.69 – 7.65 (m, 1H), 7.62 (ddd, *J* = 8.2, 2.0, 0.9 Hz, 1H), 7.35 (t, *J* = 8.1 Hz, 1H), 7.14 (ddd, *J* = 8.0, 2.0, 0.8 Hz, 1H). $^{13}$C NMR (101 MHz, DMSO-$D_6$) δ 163.69, 153.52, 149.89, 140.64, 139.61, 133.55, 130.96, 130.12, 124.71, 124.34, 120.31, 119.20. HPLC-TOF/MS: 264.9947 ([M-H]$^-$, $C_{12}H_8Cl_2N_2O^-$; calc. 264.9941).

**2-Chloro-N-(2-chlorophenyl)nicotinamide** (**N9**): Yield: 78%. Cream crystal. IR (cm$^{-1}$): 3279, 3042, 2111, 1992, 1870, 1644, 1592, 1523, 1487, 1456, 1394, 1322, 1144, 1091, 1014, 816, 755, 653, 502. $^1$H NMR (400 MHz, DMSO-$D_6$) δ 10.54, 8.88 (dd, *J* = 2.5, 0.6 Hz, 1H), 8.28 (dd, *J* = 8.3, 2.5 Hz, 1H), 7.76 – 7.70 (m, 2H), 7.64 (d, *J* = 8.3 Hz, 1H), 7.40 – 7.32 (m, 1H). $^{13}$C NMR (101 MHz, DMSO-$D_6$) δ 163.51, 153.42, 149.86, 139.58, 138.14, 130.24, 129.17 (2C), 128.28, 124.67, 122.40 (2C). HPLC-TOF/MS: 264.9943 ([M-H]$^-$, $C_{12}H_8Cl_2N_2O^-$; calc. 264.9941).

## Computational Chemistry

Gaussian software was used in the computational investigations[15,16]. The synthesized compounds were fully-optimized at the B3LYP method with 6-31+G(d) basis set in water. In this stage, conductor like polarizable continuum model (C-PCM) was used as solvent model to consider solute-solvent interactions. At the results of calculations, no imaginary frequency was observed. IR and NMR spectrum were calculated at the same level of theory. Additionally, electronic properties of these compounds are examined using contour plots of frontier molecular orbitals and moleculer electrostatic potential (MEP) map. Some utilities such as ChemDraw software was used as utility in this study[17].

## Cell Culture Studies

MCF7 (human breast cancer), HT29 (colon cancer), SNU1 (stomach cancer), SNU16 (stomach cancer), and L929 (Healthy fibroblast) obtained from the American Type Culture Collection (ATCC, Manassas, VA, USA) cell lines were used. Cells were cultured in 25 cm$^2$ flasks containing RPMI containing 10% Fetal Bovine Serum (FBS), 1% penicillin/streptomycin, and 1% L-glutamine. Cells were maintained at 37°C in a humidified atmosphere with 5% $CO_2$. Cells reaching 80% density were passaged. Cells were seeded on a 96-well plate with the number of cells in each well of 1x10$^4$ cells. The new synthesis compounds were dissolved in DMSO and diluted in culture medium before processing with a final DMSO content of 5%.

## Cell Viability Assay

MCF7, HT29, SNU1 and SNU16 cell lines were used to evaluate the anticancer activity of nine newly synthesized compounds. The XTT colorimetric method (2,3-bis-(2-methoxy-4-nitro-5-sulphophenyl)-5-[(phenylamino)carbonyl]-2H-tetrazolium hydroxide) (Biological Industries) was used to assess cell viability. MCF7, HT29, SNU1 and SNU16 cells in growth phase were seeded at a density of 1x10$^4$ cells per well in 96-well microplates prepared in RPMI 1640 culture medium (100-µL).

Processing was started after 24 hours of incubation. Synthesis compounds were administered to all cell lines individually at a dose of 40 µM. Cells were classified as control group and drug group. No drug was administered to the control group. The prepared 96-well plate was kept in the incubator and removed after 24 hours. Wells were washed with phosphate buffered saline (PBS). Then, 100 µL of phenol red-fr*ee* DMEM and 50 µL of XTT solution were added to all wells and the plates were kept at 37 °C for 4 hours. Absorbance values were determined at 450 nm using an ELISA microplate reader (Thermo Fisher Scientific, Altrincham, UK). This procedure was repeated thr*ee* times. Cell viability was accepted as 100% in the control group. Cell viability was calculated using the formula (% Cell viability = (Concentration O.D./Control O.D.) x 100). It was observed that **N4**, one of the nine compounds, had a cytotoxic effect on MCF-7 at the desired level (below 60%) in 24-hour application. Different doses (40, 20, 10, 5, 2.5 µM) of **N4** compound were applied to MCF-7 to determine the IC50 value of the **N4** compound, which has a sufficient cytotoxic effect on MCF-7 at a dose of 40 µM. The IC50 value (drug concentration causing 50% reduction in proliferation)

was calculated using Graph Prism 7 software (GraphPad). Next, the possible cytotoxic effect on the healthy connective tissue cell line L929 was investigated to investigate the selectivity of the **N4** synthesis compound to tumor cells. The **N4** compound was administered to the L929 cell line at a dose of 40 µM. The cytotoxic effects of newly synthesized **N4** on MCF-7 and L929 were compared.

**Antibacterial and antifungal activity, and Determination of MICs**

The antimicrobial activity of the synthesized complexes was examined against the microorganism; Gram-positive bacteria [*Enterococcus faecalis* (ATCC 29212), *Staphylococcus aureus* (ATCC 29213) Methicillin-resistant *S. aureus* (ATCC 43300)]; Gram-negative bacteria [*Pseudomonas aeruginosa* (ATCC 27853), *Klebsiella pneumoniae* (ATCC 700603), *Escherichia coli* (ATCC 25922)], and fungus [*Candida albicans* (ATCC 10231)]. Complexes stock solutions were dispensed at a concentration of 2 mg/ml in dimethyl sulfoxide (DMSO). The micro-broth dilution method was used to test the Minimum Inhibitory Concentration (MIC) values of compounds[18]. The concentrations of compounds were prepared by serial dilution in Mueller Hinton Broth (MHB). For positive control; ciprofloxacin (to bacteria), and fluconazole (to fungus) were used as antimicrobials. The microplates were incubated at 37°C for 24 hours. All experiments were repeated 3-times.

**Biofilm inhibition concentration (BIC) assay**

A 96-well microtiter plate method was used to test the biofilm inhibition potential of the synthesized compounds[19]. The microorganisms used in the assay were cultured overnight in Tryptic Soy Broth (TSB) (supplemented with 2% glucose). Test compounds were prepared at Minimum Inhibition Concentration (MIC) values ranging from 500 to 1000 µg/ml. The initial inoculum was mixed with bacterial suspensions with a concentration of $5x10^5$ CFU/mL. 100 µL of compound solution and 100 µL of McFarland 0.5 ($10^8$ CFU/ml) turbid bacteria suspension were added to microplates (96-well, U-bottom). Only 200 µL of bacterial suspension was added to the wells as a positive control. The microplates were then incubated at 37 °C for 48 hours. After this time, the wells of the microplate were washed 3 times with phosphate-buffered saline (PBS). Thus, non-adherent bacteria were removed. The biofilm structure in the wells was fixed with 95% methyl alcohol for 15 minutes. The microplates were dried at room temperature. Next, 200 µl of 0.1% crystal violet was added to the wells and left for 30 min. The wells were washed 3-times with distilled water to remove excess dye, and the microplates were dried. 33% acetic acid solution was added to dissolve the attached dye in the wells. After 20 minutes, biofilm inhibition was measured at 570 nm with a UV-Vis spectrophotometer (Bio-Tek, Winooski, USA). The biofilm inhibition rate was calculated according to the formula given below. All experiments were repeated 3 times.

$$\% \text{ Inhibition} = 100\text{-}\left(\frac{OD570\ sample}{OD570\ control}\ X\ 100\right)$$

**Results and Discussion**

**Optimized Structures**

The synthesized compounds are optimized at B3LYP/6-31+G(d) level in the water. The ground state structure of these compounds are showed in Fig. 3. In addition, selected geometric parameters which are bond length (Å), bond angle (deg.) and dihedral angle (deg.) are given in Table 1.

According to Table 1, geometric parameters are close to each other. However, the structures of studied compounds are not planar. Almost, the benzene rings in the studied compounds stand perpendicular to each other.

**Experimental and Computational IR Spectra**

The IR spectrum is a fundamental technique for determining the functional group and is essential for the characterization of chemicals. The vibrational frequencies of the studied compounds were obtained both experimentally and computationally. Experimental results are given in the below sections. In this section, assignments are made by comparing computational and experimental results with each other. The IR results are given in Table 2 for studied compounds.

According to Table 2, some numerical differences are there in calculated and experimental frequencies. The main reason for this difference is that the calculated frequencies are harmonic values. However, regression coefficient is calculated at nearly 0.997 for each data set. Labeling of experimental results along with computational IR results is performed. In addition, it is observed that the results obtained are compatible with the IR datasets.

**NMR Spectra**

Dimethyl sulfoxide-d6 are used as the deuterated solvent for the synthesized compounds. In the $^1$H-

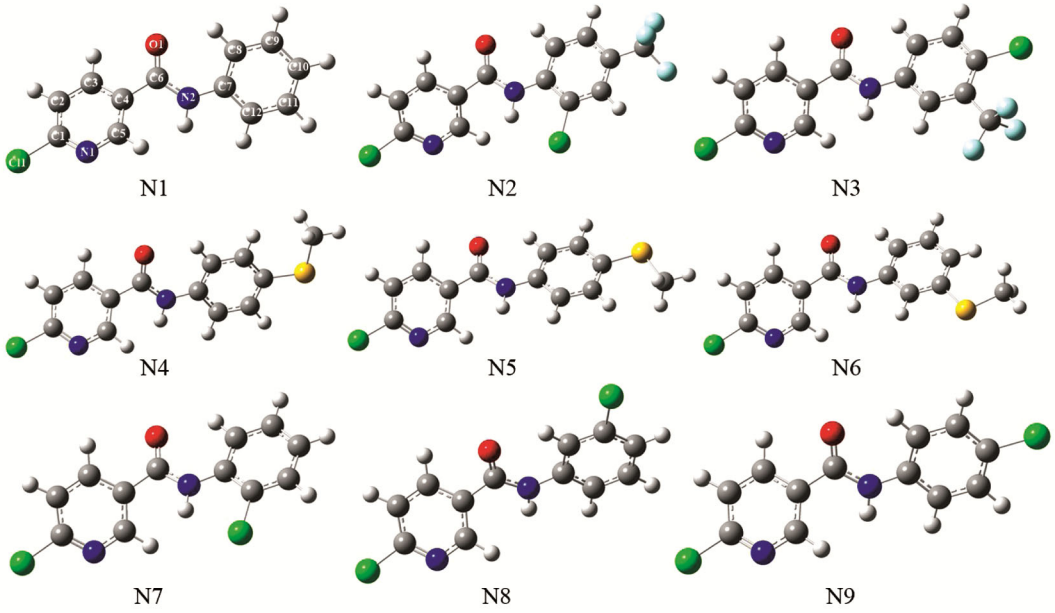


Fig. 3 — The optimized structure of examined nicotinamide derivatives

Table 1 — The geometric parameters of synthesized compounds at B3LYP/6-31+G(d) level.

| Assignments | N1 | N2 | N3 | N4 | N5 | N6 | N7 | N8 | N9 |
|---|---|---|---|---|---|---|---|---|---|
| Bond Lengths (Å) | | | | | | | | | |
| C1-C2 | 1.398 | 1.398 | 1.398 | 1.398 | 1.398 | 1.398 | 1.398 | 1.398 | 1.398 |
| C1-Cl1 | 1.762 | 1.761 | 1.761 | 1.763 | 1.763 | 1.762 | 1.762 | 1.762 | 1.762 |
| C1-N1 | 1.322 | 1.322 | 1.322 | 1.321 | 1.322 | 1.322 | 1.322 | 1.322 | 1.322 |
| N1-C5 | 1.342 | 1.342 | 1.342 | 1.342 | 1.342 | 1.342 | 1.342 | 1.342 | 1.342 |
| C4-C6 | 1.403 | 1.500 | 1.500 | 1.502 | 1.502 | 1.502 | 1.501 | 1.501 | 1.502 |
| C6-O1 | 1.235 | 1.230 | 1.232 | 1.236 | 1.236 | 1.234 | 1.233 | 1.234 | 1.234 |
| C6-N2 | 1.367 | 1.376 | 1.371 | 1.366 | 1.366 | 1.368 | 1.371 | 1.369 | 1.368 |
| N2-C7 | 1.415 | 1.400 | 1.408 | 1.415 | 1.414 | 1.414 | 1.407 | 1.411 | 1.412 |
| Bond Angle (deg.) | | | | | | | | | |
| Cl1-C1-C2 | 118.8 | 118.8 | 118.8 | 118.8 | 118.8 | 118.8 | 118.8 | 118.8 | 118.8 |
| C1-C2-C3 | 117.0 | 117.0 | 117.0 | 117.0 | 117.0 | 117.0 | 117.0 | 117.0 | 117.0 |
| Cl1-C1-N1 | 116.3 | 116.2 | 116.3 | 116.3 | 116.3 | 116.3 | 116.3 | 116.3 | 116.3 |
| C3-C4-C6 | 118.6 | 118.5 | 118.6 | 118.6 | 118.6 | 118.7 | 118.6 | 118.5 | 118.5 |
| C4-C6-N2 | 115.4 | 115.2 | 115.3 | 115.5 | 115.4 | 115.2 | 115.2 | 115.4 | 115.4 |
| C4-C6-O1 | 120.4 | 120.9 | 120.8 | 120.5 | 120.5 | 120.5 | 120.6 | 120.6 | 120.6 |
| O1-C6-N2 | 124.1 | 123.8 | 123.7 | 123.9 | 124.0 | 124.1 | 124.1 | 123.8 | 123.9 |
| C6-N2-C7 | 129.2 | 128.7 | 128.6 | 129.0 | 129.1 | 129.0 | 128.8 | 129.1 | 129.0 |
| Dihedral Angle (deg.) | | | | | | | | | |
| Cl1-C1-C2-C3 | -179.8 | 179.8 | 179.8 | -179.8 | 179.8 | 179.8 | 179.8 | -179.8 | -179.8 |
| Cl1-C1-N1-C5 | 179.4 | -179.3 | -179.3 | 179.4 | -179.3 | -179.3 | -179.4 | 179.3 | 179.3 |
| C1-N1-C5-C4 | 0.0 | -0.10 | -0.12 | 0.06 | -0.06 | -0.12 | -0.10 | 0.08 | 0.09 |
| C4-C6-N2-C7 | -177.6 | 176.1 | 177.1 | -177.6 | 177.6 | 177.4 | 176.7 | -177.4 | -177.6 |
| C5-C4-C6-O1 | -147.9 | 148.8 | 148.4 | -147.9 | 148.3 | 147.8 | 148.4 | -149.2 | -148.4 |
| C6-N2-C7-C12 | -174.1 | 173.9 | 174.7 | -173.4 | 173.4 | 171.1 | 172.5 | -175.6 | -175.2 |

NMR spectra of the synthesized compounds, the proton of amide group give a singlet in the range of 10.35 – 10.77 ppm. Calculated chemical shift value of proton of amide group is obtained in the range of 9.2 – 10.7 ppm at same level of theory. In the $^{13}$C-NMR spectra, the carbonyl group are resonated in the range of 163.2 – 163.9 ppm. Chemical shift value of this atom is calculated in the range of 159.4 – 160.5 ppm.

Table 2 — Vibrational frequencies ($cm^{-1}$) of some functional groups in studied compounds

| Assignments | N1 | | N2 | | N3 | | N4 | |
|---|---|---|---|---|---|---|---|---|
| | Exp. | Calc. | Exp. | Calc. | Exp. | Calc. | Exp. | Calc. |
| $\nu_{NH}$ | 3307 | 3601 | 3319 | 3580 | 3334 | 3598 | 3314 | 3601 |
| $\nu_{CH}$ | 3045 | 3197 | 3078 | 3199 | 3079 | 3196 | 3056 | 3198 |
| $\nu_{C=O}$ | 1647 | 1697 | 1667 | 1715 | 1686 | 1706 | 1653 | 1693 |
| $\nu_{C-N}$ | 1495 | 1576 | 1458 | 1562 | 1477 | 1566 | 1522 | 1561 |
| $\nu_{C=C}$ | 1366 | 1316 | 1398 | 1318 | 1320 | 1317 | 1319 | 1316 |
| $\nu_{C-Cl}$ | 683 | 758 | 703 | 749 | 754 | 738 | 761 | 763 |
| | N5 | | N6 | | N7 | | N8 | |
| | Exp. | Calc. | Exp. | Calc. | Exp. | Calc. | Exp. | Calc. |
| $\nu_{NH}$ | 3271 | 3604 | 3304 | 3597 | 3280 | 3583 | 3281 | 3603 |
| $\nu_{CH}$ | 3043 | 3197 | 3065 | 3196 | 3060 | 3198 | 3069 | 3199 |
| $\nu_{C=O}$ | 1644 | 1693 | 1667 | 1700 | 1642 | 1705 | 1647 | 1702 |
| $\nu_{C-N}$ | 1583 | 1564 | 1585 | 1572 | 1585 | 1566 | 1580 | 1570 |
| $\nu_{C=C}$ | 1329 | 1316 | 1327 | 1316 | 1312 | 1316 | 1324 | 1322 |
| $\nu_{C-Cl}$ | 807 | 763 | 778 | 771 | 737 | 764 | 795 | 762 |
| | N9 | | | | | | | |
| | Exp. | Calc. | | | | | | |
| $\nu_{NH}$ | 3279 | 3605 | | | | | | |
| $\nu_{CH}$ | 3042 | 3197 | | | | | | |
| $\nu_{C=O}$ | 1644 | 1700 | | | | | | |
| $\nu_{C-N}$ | 1592 | 1568 | | | | | | |
| $\nu_{C=C}$ | 1322 | 1316 | | | | | | |
| $\nu_{C-Cl}$ | 755 | 762 | | | | | | |

**Electronic Properties**

Determination of electronic properties is essential for compounds. Computationally, the field of application of the studied compounds can be easily determined using contour plots of the boundary molecular orbital and molecular electrostatic potential (MEP). In this study, contour plots of boundary molecular orbitals, which are HOMO and LUMO, are calculated and shown in Fig. 4.

According to Fig. 4, HOMO electrons are delocalized mainly on the benzene ring in the structure of the studied compound. At this point, it is observed that π electrons play an important role. In the LUMO graph, the electrons are mainly localized over the entire structure of the molecule. The MEP map can be used to determine the electronic properties of compounds. The contour plot of the boundary molecular orbitals shows the specific area that can be active, while the MEP maps show the regions that can interact on the surface of the compound. MEP maps of the investigated compounds were calculated and shown in Fig. 5.

To predict reactive sites of electrophilic or nucleophilic attack for the mentioned molecules, the MEP at the B3LYP/6-31+G(d) optimized geometry was calculated. The negative (red and yellow) regions of the MEP are related to nucleophilic activity as environment of oxygen atoms in carboxyl grops and the positive (blue) regions to electrophilic activity, as shown in Fig. 5.

**Anticancer Activities**

In the scope of the study, human breast cancer (MCF-7), human colon cancer (HT-29) and human gastric cancer (SNU1, SNU16) cell lines were used in *in vitro* studies to evaluate the anticancer activities of 9 newly synthesized compounds. In the first step, all compounds were applied to all 4 cell lines at a constant concentration of 40 μM. Cell viability percentages were calculated by XTT colorimetric method 24 hours after the application. The study was repeated 3 times and the averages of the results were calculated. Results below 60% were considered significant. As a result of the examinations, it was determined that other compounds, except **N4**, did not show the desired cytotoxic effect. However, it was determined that **N4** provided 55.11% viability on the breast cancer cell line MCF7 and showed cytotoxic effect at the desired level. Based on all these results, **N4** was chosen for further studies (Table 3).

In the next step of the study, the IC50 value of the **N4** compound, which was effective in the MCF-7 cell line, was determined. **N4** compound was applied to the MCF-7 cell line at doses of 2.5 μM, 5 μM, 10 μM,

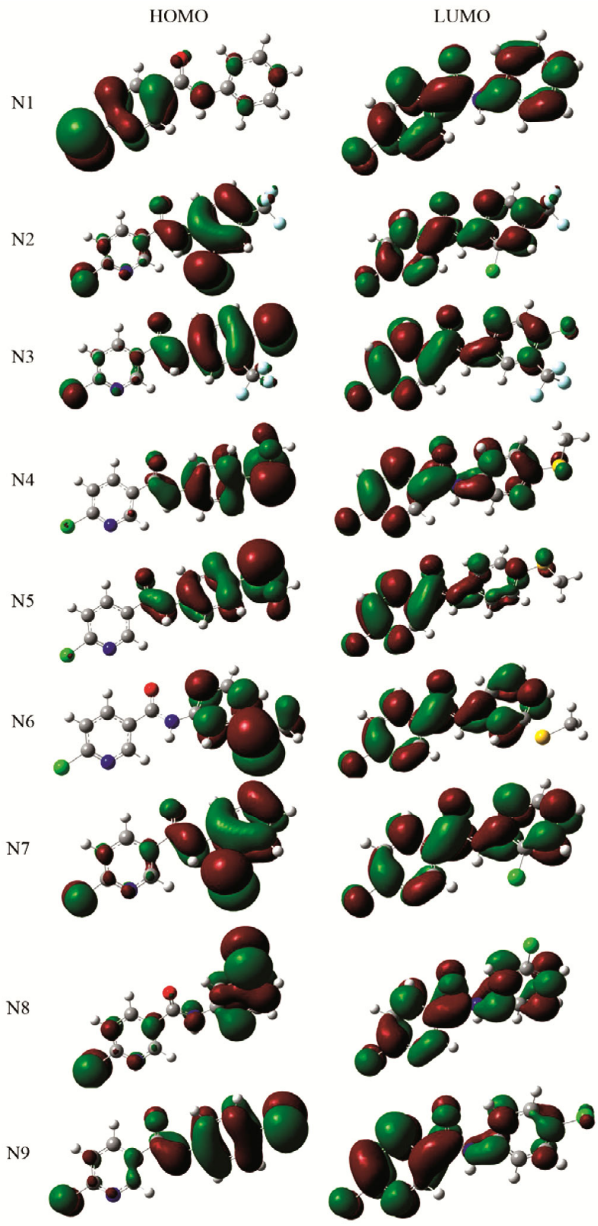


Fig. 4 — Contour diagram of frontier molecular orbitals

20 µM and 40 µM. Cell viability was determined by XTT after 24 hours of administration. The mean cell viability rates obtained after three replicates were calculated and the IC50 value was found to be 12.1 µM (Table 4).

In the final phase of the *in vitro* part of the study, the effect of the potential cytotoxicity of **N4** on the healthy fibroblast cell line L929 was examined at a high dose of 40µM. As a result, with the application of the newly synthesized **N4** compound at a dose of 40µM for 24 hours, it caused 55.11% cell viability in the breast cancer cell line MCF-7, but 89.7% cell viability in the healthy fibroblast cell line L929. In the light of all these results, it was determined that **N4** had a more specific cytotoxic effect on MCF7 than on healthy cells.

## Antibacterial, Antifungal and Antibiofilm Activities

Biofilms are defined as clumps of microorganisms in which bacteria adhere to each other and/or a surface and are embedded in a matrix of polymeric substances that they produce from their organisms and secrete out of the cell. By means of this structure, microorganisms are thousands of times more resistant to antibiotics and other antimicrobials than planktonic (free-living) organisms[20].

Biofilm-associated infections are severe and recurrent diseases that are difficult to treat. Therefore, there is need for new strategies for the prevention and treatment of the proliferation of bacterial biofilms urgently. The antibacterial and antibiofilm activity of studied compounds are tested *in vitro* against six standard bacterial strains and one fungus.

When Table 5 was examined according to the results of the research, it was determined that the most effective compounds on microorganisms were **N2** and **N3**, and the weakest one is **N1**. Other compounds also had moderate to strong (in varying levels) antimicrobial activity. *E. faecalis* (ATCC 29212) strain was determined as the most sensitive microorganism to the compounds.

Due to the antimicrobial properties of vitamin B3 (nicotinamide and nicotinic acid) and vitamin B6 (pyridoxine) derivatives, it attracts the attention of experts in the treatment of common and life-threatening microbial infections that are tolerant or resistant to current drugs[21]. Adamiec et al. examined the antibacterial activity of the 1-methyl-N'-(hydroxymethyl)nicotinamide chloride (MNAF+) compound against *E. faecalis, S. aureus, E. coli*, and *P. aeruginosa* bacteria, and it was determined that it was significantly effective. At the same time, in parallel with the results of this study, they reported that the most sensitive bacteria to the compounds was *E. faecalis*[22]. In another study, it was determined that pyridoxin and nicotinium dithiophosphate compounds had a strong antibacterial activity; (10–20 µM) against *Staphylococci* bacteria; and at increasing concentrations (MIC≥320µM) against *P. aeruginosa* and *K. Pneumonia.* Venkatasubramanian et al. reported that new nicotinamide-thiazole derivatives

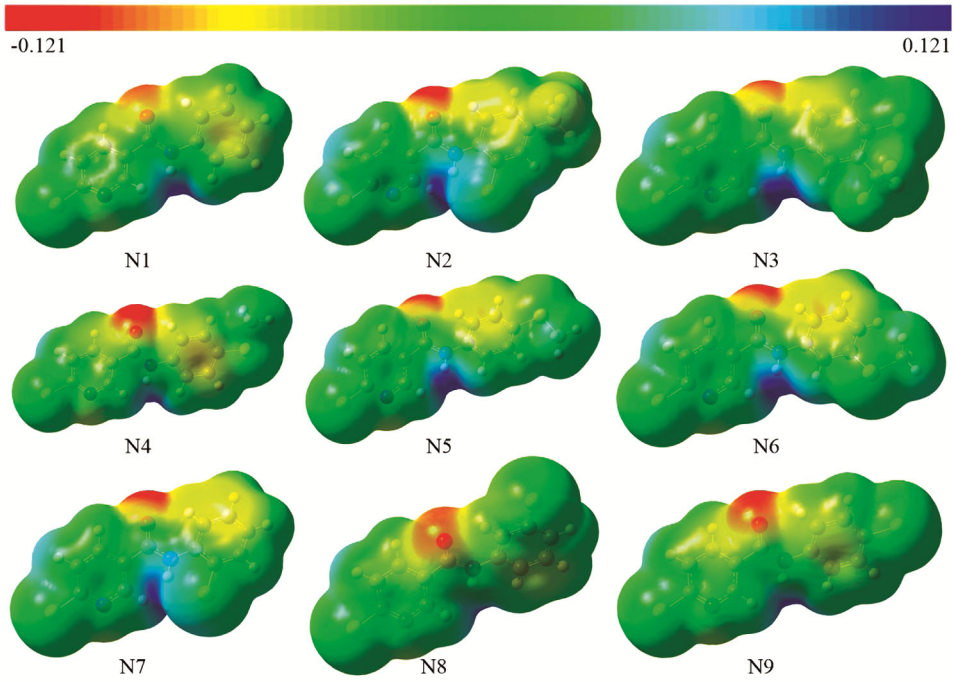


Fig. 5 — MEP maps of the studied compounds

Table 3 — XTT results obtained after 24 hours application of studied compounds at 40 µM dose to four different cell lines

| Cell Line | N1 | N2 | N3 | N4 | N5 | N6 | N7 | N8 | N9 |
|---|---|---|---|---|---|---|---|---|---|
| MCF-7 | 101.18 | 80.79 | 60.47 | 55.11* | 92.66 | 77.49 | 100.59 | 74.78 | 98.38 |
| HT-29 | 96.73 | 87.72 | 92.80 | 71.32 | 97.83 | 90.35 | 88.61 | 94.66 | 89.54 |
| SNU1 | 97.15 | 104.55 | 97.47 | 106.30 | 115.74 | 107.22 | 105.98 | 107.01 | 99.19 |
| SNU16 | 104.16 | 97.12 | 101.02 | 61.89 | 105.17 | 106.08 | 104.82 | 90.27 | 87.91 |

* Significant result below 60%.
MCF-7: Breast cancer cell line, HT-29: Colon cancer cell line, SNU1: Gastric cancer cell line, SNU16: Gastric cancer cell line.

showed potent antimicrobial activity against the microbial pathogens tested[23].

In this study, studied compounds are determined to have moderate and strong antibiofilm activities. When Table 6 was examined, the antibiofilm activity against all tested pathogenic microorganisms was found to be 3.2% to 78.3% at ½ MIC concentrations of the synthesized compounds. The microorganisms with the strongest inhibition value against biofilm formation of the tested compounds; *Mrsa* (69.6-78.3%), and *C. albicans* (54.1-72.7%). The microorganism with the lowest activity of the compounds was determined as *K. pneumoniae* (3.2-17.1%).

Sihih et al. reported that the nicotinamide destroyed the biofilm structure of Cutibacterium acnes bacteria and prevented biofilm formation[24]. In another study, it was reported that pyridine nicotinamide derivatives caused destabilization in EPS produced by *Micrococcus luteus* and *S. aureus* species, destroying the biofilm structure and causing the bacteria to become planktonic, and thus these compounds acted as an antibiofilm agent[25].

Table 4 — Effect of N4 synthesis compound at 5µM, 10µM, 20µM, 40µM, 80µM doses in MCF-7 cell line and determination of IC50 value.

| | | MCF-7(Brest cancer) |
|---|---|---|
| N4 Dose | n | Mean |
| Control | 3 | 100 |
| 2.5 µM | 3 | 134.83 |
| 5 µM | 3 | 113.75 |
| 10 µM | 3 | 105.68 |
| 20 µM | 3 | 85.73 |
| 40 µM | 3 | 55.09 |
| | IC50: 12.1 µM | |

MCF-7: Breast cancer cell line, N4: New synthesis compound, IC50: Drug concentration causing 50% reduction in proliferation

Our results indicate that the newly synthesized and characterized compounds have remarkable antibacterial and antifungal activity. It was determined that the most effective antimicrobial compunds were **N2** and **N3**, and

the lowest antimicrobial compound was **N1**. Furthermore, these compounds prevented biofilm formation at moderate to high levels. Based on these results, these compounds are thought to encourage the development of novel antibiofilm agents.

## *In silico* Analyses

### Pharmacophore Model

Pharmacophore is related with the description of the molecular properties in the recognition of molecule as ligand. Generally, pharmacophore models may contain hydrophobic centroids, aromatic rings, hydrogen bond acceptors or donors, cations, and anions [Wermuth CG, Ganellin CR, Lindberg P, Mitscher LA (1998). "Glossary of terms used in medicinal chemistry (IUPAC Recommendations 1998)". Pure and Applied Chemistry. 70 (5): 1129–1143. doi:10.1351/pac199870051129.]. Pharmacophore analyses of the studied compounds are performed using Maestro 12.2 software and totally twenty pharmacophore models are derived. The best one is represented in the Fig. 6.

Table 5 — Antimicrobial screening data of the compounds (MIC in μM)

| Compd* | Antibacterial activity | | | | | | Antifungal activity |
|---|---|---|---|---|---|---|---|
| | Sa | Mrsa | Ec | Kp | Pa | Ef | Ca |
| N1 | 85,9 | 85,9 | 85,9 | 85,9 | 85,9 | 42,9 | 85,9 |
| N2 | 59,6 | 59,6 | 59,6 | 59,6 | 59,6 | 29,8 | 59,6 |
| N3 | 59,6 | 59,6 | 59,6 | 59,6 | 59,6 | 29,8 | 59,6 |
| N4 | 66,5 | 66,5 | 66,5 | 66,5 | 66,5 | 66,5 | 66,5 |
| N5 | 71,7 | 71,7 | 71,7 | 71,7 | 71,7 | 71,7 | 71,7 |
| N6 | 71,7 | 71,7 | 71,7 | 71,7 | 71,7 | 71,7 | 71,7 |
| N7 | 74,8 | 74,8 | 74,8 | 74,8 | 74,8 | 37,4 | 74,8 |
| N8 | 74,8 | 74,8 | 74,8 | 74,8 | 74,8 | 37,4 | 74,8 |
| N9 | 74,8 | 74,8 | 74,8 | 74,8 | 74,8 | 37,4 | 74,8 |
| Ciprofloxacin | 0.5 | 1.0 | 2.0 | 0.25 | 0.5 | 1.0 | |
| Flucanazole | | | | | | | 5 |

Sa*; Staphylococcus aureus* (ATCC 29213)*,* Mrsa; Methicillin-resistant *S. aureus* (ATCC 43300), Ef; *Enterococcus faecalis* (ATCC 29212), Ec; *Escherichia coli* (ATCC 25922), Pa; *Pseudomonas aeruginosa* (ATCC 27853), Kp; *Klebsiella pneumoniae* (ATCC 700603), Ca; *Candida albicans* (ATCC10231)

Table 6 — Biofilm inhibition assay of synthesized compounds (MIC/2 in μM)

| | Antibiofilm inhibition (%) | | | | | | |
|---|---|---|---|---|---|---|---|
| Compd* | Sa | Mrsa | Ec | Kp | Pa | Ef | Ca |
| N1 | 25.0±0.11 | 69.8±0.05 | 6.4±0.12 | 3.2±0.24 | 25.0±0.19 | 36.9± 0.45 | 67.4±0.05 |
| N2 | 24.4±0.08 | 73.8±0.27 | 5.3±0.21 | 5.7±0.09 | 31.8±0.04 | 29.4± 0.01 | 67.3± 0.07 |
| N3 | 20.3±0.48 | 73.6±0.35 | 7.6±0.14 | 15.6±0.63 | 8.5±0.54 | 32.8± 0.33 | 71.6± 0.15 |
| N4 | 24.1±0.07 | 69.6±0.09 | 14.1±0.06 | 10.0±0.18 | 16.6±0.33 | 36.1± 0.24 | 72.7± 0.14 |
| N5 | 21.7±0.14 | 70.1±0.11 | 8.3±0.06 | 3.4±0.17 | 29.7±0.09 | 32.7± 0.03 | 68.5± 0.06 |
| N6 | 23.7±0.05 | 70.6±0.08 | 7.9±0.07 | 4.6±0.3 | 32.1±0.08 | 26.8±0.24 | 67.0± 0.04 |
| N7 | 21.2±0.14 | 70.1±0.11 | 12.9±0.53 | 13.7±0.32 | 5.6±0.62 | 30.6±0.18 | 68.1± 0.4 |
| N8 | 43.0±0.38 | 78.3±0.34 | 34.1±0.4 | 3.7±0 | 31.0± 0.83 | 48.1± 0.12 | 64.9± 0.23 |
| N9 | 31.0±0.42 | 78.0±0.4 | 22.4±0.3 | 12.8±0.65 | 33.8± 0.82 | 46.8± 0.54 | 54.1± 0.2 |

Sa*; Staphylococcus aureus* (ATCC 29213)*,* Mrsa; Methicillin-resistant *S. aureus* (ATCC 43300), Ef; *Enterococcus faecalis* (ATCC 29212), Ec; *Escherichia coli* (ATCC 25922), Pa; *Pseudomonas aeruginosa* (ATCC 27853), Kp; *Klebsiella pneumoniae* (ATCC 700603), Ca; *Candida albicans* (ATCC10231)

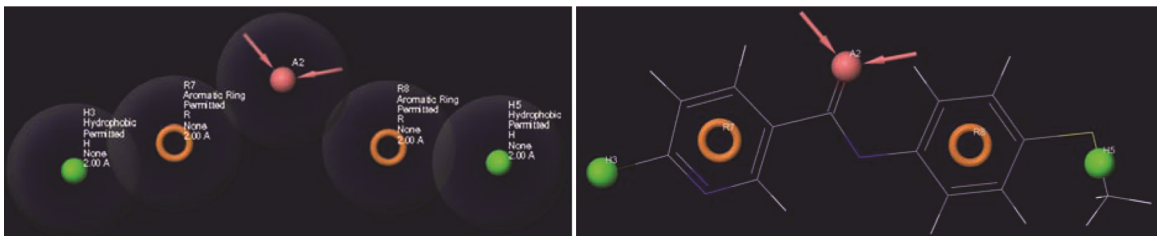


Fig. 6 — The pharmacophore model

This model is derived by taking of N4 compound as reference substance. In this model, there are two aromatic rings, two hydrophobic sites and H acceptor. In the derivation of model, all compounds are taken in to consideration however N4 compound is selected as reference material by software. The pharmacophore map is represented in Fig. 6, too. In drug design, new atom or atoms groups can be added to these molecule unless the pharmacophore map is not changed.

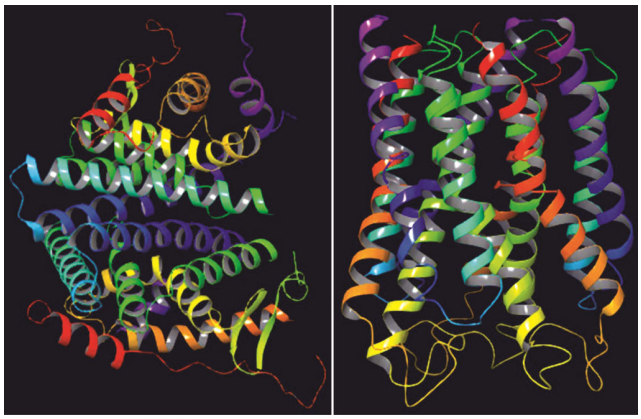


Fig. 7 — The structure of target proteins, 6VGH and 3DWW

## Molecular Docking

Biological activity of studied compounds can be determined by experimental and computational techniques. In computational analyses, many researchers have used the quantum chemical descriptors and molecular docking calculations have been popular in the last years. In this study, molecular docking calculations are performed against estrogen receptor and protoglastin. These proteins are mainly expressed in breast cancer which is the most common cancer type. These proteins are downloaded as 6VGH and 3DWW from protein data bank web tool for estrogen receptor and prostaglandin, respectively. *p*H is selected as 7±2 in the whole calculation. The protein structure of them are represented in Fig. 7.

Additionally, studied compounds and target proteins are minimized at OPLS4 method. The receptor binding domain (RBD) of these proteins are represented in Fig. 8. (x/y/z) coordinate of the 6VGH and 3DWW are (-32.97/-3.45/-18.69) and (85.45/-41.29/22.96), respectively. Furthermore, the significant aminoacids in these regions are represented in Fig. 8, too.

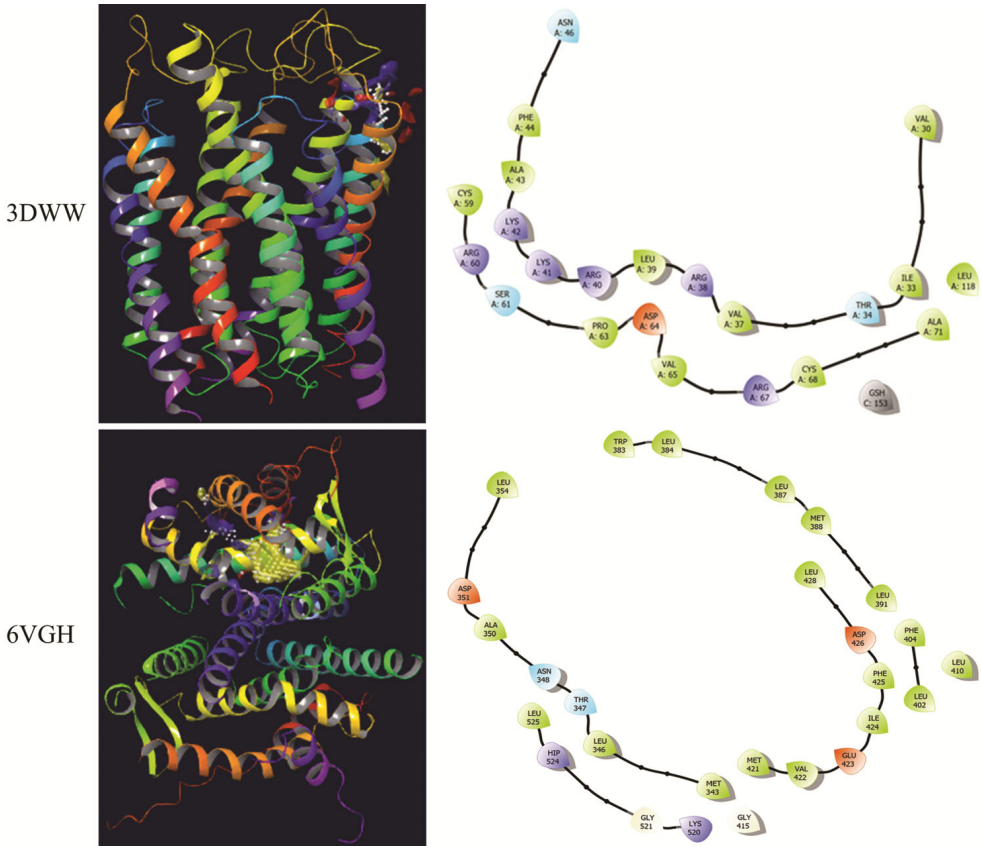


Fig. 8 — The RBD of target protein and the related amino acid in these domains.

Table 7 — The docking calculations results

| Compd | DS[a] | $E_{vdW}$[a] | $E_{Coul}$[a] | $E_{Total}$[a] |
|---|---|---|---|---|
| For 6VGH | | | | |
| N1 | -6.446 | -25.740 | -1.490 | -27.230 |
| N2 | -4.933 | -28.867 | -2.403 | -31.270 |
| N3 | -5.863 | -28.669 | -1.978 | -30.647 |
| N4 | -8.104 | -31.054 | -1.112 | -32.166 |
| N5 | -5.128 | -27.801 | -1.860 | -29.661 |
| N6 | -6.188 | -29.655 | -0.761 | -30.415 |
| N7 | -6.246 | -33.148 | -3.243 | -36.391 |
| N8 | -4.493 | -31.424 | -1.179 | -32.603 |
| N9 | -6.932 | -26.838 | -0.787 | -27.625 |
| For 3DWW | | | | |
| N1 | -2.393 | -30.270 | -2.397 | -32.667 |
| N2 | -1.985 | -33.741 | -3.410 | -37.151 |
| N3 | -2.574 | -30.786 | -2.619 | -33.405 |
| N4 | -1.781 | -29.941 | -3.971 | -33.913 |
| N5 | -0.058 | -30.057 | -2.009 | -32.066 |
| N6 | -3.531 | -26.301 | -5.487 | -31.787 |
| N7 | -2.535 | -30.870 | -2.109 | -32.980 |
| N8 | -1.920 | -25.440 | -2.903 | -28.343 |
| N9 | -2.101 | -25.938 | -3.829 | -29.767 |

[a] in kcal/mol

The biological activity of studied compounds against are determined by molecular docking calculations. These calculations are performed and docking score (DS), van der Walls interaction energy ($E_{vdW}$), the Coulomb interaction energy ($E_{Coul}$) and total interaction energy ($E_{Total}$) are given in Table 7.

According to Table 7, studied compounds exhibited better results in estrogen receptor than that of prostaglandin. For prostaglandin protein, obtained results cannot be accepted as good results. The inhibition efficiency of studied compounds seems bad. However, the related compounds have good inhibition properties in estrogen receptor. The best results are obtained in N4 compound. The docking score of this compound is calculated as -8.104 kcal/mol. This result implies that there is well key-lock harmony between ligand and receptor. Furthermore, the total interaction energy of related compounds are similar to each other and it is observed that there is no any significant difference. Finally, it can be said that inhibition properties of studied compounds are good in estrogen receptor that those of prostaglandin and N4 is found as the best inhibitor candidate for the estrogen receptor.

**Absorption, Distribution, Metabolism and Excretion (ADME) Analysis**

ADME analysis gives essential clues about pharmacokinetics and pharmacology properties of pharmaceutical compound within an organism. The whole criteria affect drug levels and drug exposure kinetics to tissues and so affect the performance and pharmacological activity of the drug candidates. ADME calculations are performed using Maestro 12.8 software and QikProp descriptors of studied compounds are calculated. Selected some QikProp parameters are given in Table 8.

According to Table 8, calculated parameters are generally in good agreement with the recommended value for each parameter. These parameters reveal the drug-likeness properties of the investigated compounds. Especially, these compounds have skin permeability, MDCK cell permeability, Caco-2 cell permeability, brain/blood permeability. Additionally, some compounds can take part in metabolic reactions which is undesirable. In this stage, only compound N5 is out of point and it can be taken out of study. On the other hand, if it will be in the study, the dose of the drugs taken into the body should be adjusted. As a result, all results seems good in ADME analysis.

Table 8 — Calculated QikProp parameters of studied compounds

| Parameters[a] | N1 | N2 | N3 | N4 | N5 | N6 | N7 | N8 | N9 | RV[b] |
|---|---|---|---|---|---|---|---|---|---|---|
| Stars | 0 | 1 | 1 | 0 | 1 | 0 | 0 | 0 | 0 | 0-5 |
| Amine | 0 | 0 | 0 | 0 | 0 | 0 | 0 | 0 | 0 | 0-1 |
| rtvFG | 0 | 0 | 0 | 0 | 0 | 0 | 0 | 0 | 0 | 0-2 |
| SASA | 462.85 | 533.39 | 531.83 | 529.13 | 529.50 | 530.64 | 484.84 | 487.47 | 487.00 | 300.0-1000.0 |
| FOSA | 0.00 | 0.66 | 0.57 | 89.05 | 89.04 | 87.46 | 0.000 | 0.000 | 0.000 | 0.0-750.0 |
| FISA | 69.76 | 68.42 | 69.88 | 69.82 | 69.82 | 67.38 | 72.96 | 69.82 | 69.76 | 7.0-330.0 |
| PISA | 319.05 | 215.09 | 222.16 | 254.75 | 255.11 | 260.23 | 278.33 | 272.13 | 271.69 | 0.0-450.0 |
| WPSA | 74.03 | 249.21 | 239.21 | 115.51 | 115.51 | 115.56 | 133.54 | 145.51 | 145.54 | 0.0-175.0 |
| donorHB | 1 | 1 | 1 | 1 | 1 | 1 | 1 | 1 | 1 | 0.0-6.0 |
| AccptHB | 3.5 | 3.5 | 3.5 | 4 | 4 | 4 | 3.5 | 3.5 | 3.5 | 2.0-20.0 |
| QPpolrz | 25.69 | 30.26 | 30.15 | 29.41 | 29.42 | 29.55 | 27.07 | 27.03 | 27.00 | 13.0-70.0 |
| QPPCaco | 2159.49 | 2223.36 | 2153.68 | 2156.73 | 2156.70 | 2274.63 | 2013.57 | 2156.51 | 2159.35 | <25 poor >500 great |
| QPlogBB | 0.001 | 0.407 | 0.368 | 0.001 | 0.001 | 0.023 | 0.108 | 0.159 | 0.161 | -3.0- 1.2 |
| QPPMDCK | 2892.62 | 10000 | 10000 | 4874.48 | 4874.52 | 5166.73 | 5681.23 | 7115.50 | 7128.56 | <25 poor >500 great |
| QPlogKp | -1.48 | -1.83 | -1.83 | -1.62 | -1.62 | -1.55 | -1.69 | -1.65 | -1.65 | -8.0- -1.0 |
| metab | 2 | 1 | 2 | 1 | 0 | 2 | 2 | 2 | 1 | 1-8 |
| QPlogKhsa | -0.07 | 0.28 | 0.27 | 0.10 | 0.10 | 0.11 | 0.03 | 0.03 | 0.03 | -1.5- 1.5 |
| Percent Human-Oral Absorption | 100 | 100 | 100 | 100 | 100 | 100 | 100 | 100 | 100 | >80% is high <25% is poor |
| PSA | 48.00 | 48.41 | 48.01 | 47.96 | 47.96 | 48.01 | 46.91 | 48.04 | 48.00 | 7.0- 200.0 |
| RuleOfFive | 0 | 0 | 0 | 0 | 0 | 0 | 0 | 0 | 0 | Max is 4 |
| RuleOfThree | 0 | 0 | 0 | 0 | 0 | 0 | 0 | 0 | 0 | Max is 3 |

[a]**Stars**: Number of property or descriptor values that fall outside the 95% range of similar values for known drugs; **Amine**: Number of non-conjugated amine groups; **rtvFG**: Number of reactive functional groups; **SASA**: Total solvent accessible surface area; FOSA: Hydrophobic component of the SASA; **FISA**: Hydrophilic component of the SASA; **PISA**: π (carbon and attached hydrogen) component of the SASA; **WPSA**: Weakly polar component of the SASA; **donorHB**: Estimated number of hydrogen bonds that would be donated; **AccptHB**: Estimated number of hydrogen bonds that would be accepted; **QPpolrz**: Predicted polarizability in cubic angstroms; **QPPCaco**: Predicted apparent Caco-2 cell permeability in nm/sec; **QPlogBB**: Predicted brain/blood partition coefficient; **QPPMDCK**: Predicted apparent MDCK cell permeability in nm/sec; **QPlogKp**: Predicted skin permeability; **metab**: Number of likely metabolic reactions; **QPlogKhsa**: Prediction of binding to human serum albumin; **PercentHuman-OralAbsorption**: Predicted human oral absorption on 0 to 100% scale; **PSA**: Van der Waals surface area of polar nitrogen and oxygen atoms; **RuleOfFive**: Number of violations of Lipinski's rule of five; **RuleOfThree**: Number of violations of Jorgensen's rule of three.
[b] RV: Recommended Value

## Conclusions

In our study, nine new nicotinamide derivative compounds were synthesized. Characterization of synthesized compounds was done by *in silico* analysis. The anticancer activity of nine compounds was investigated in four different cancer types (MCF-7, HT-29, SNU1 and SNU16) and healthy fibroblast cell line (L929). It was determined that N4, one of the new synthesis compounds, has the desired cytotoxic effect on the human breast cancer cell line MCF-7. The IC50 value was calculated. It was observed that the N4 compound at the dose effective against MCF-7 did not have a serious cytotoxic effect on healthy fibroblate cells (L929). In another phase of the study, its antibacterial effect in six bacterial species, its antifungal effect in one fungal species and its antibiofilm effect were investigated. It was determined that they have remarkable Antibacterial, Antifungal and Antibiofilm activities, especially N2 and N3 compounds. In the light of all these analyzes, it has been seen that N4, one of the newly synthesized nicotinamide derivative compounds, is promising in the treatment of breast cancer. However, these results, which are the first in the literature and revealed by *in silico* and *in vitro* methods, need to be supported by *in vivo* and clinical studies.

## Supplementary Information

Supplementary information is available in the website http://nopr.niscpr.res.in/handle/ 123456789/58776.

## Acknowledgment

This work is supported by the Scientific Research Project Fund of Sivas Cumhuriyet University under the project number RGD-036. This research was made possible by TUBITAK ULAKBIM, High Performance, and Grid Computing Center (TR-Grid e-Infrastructure).

## References

1 Wu J, Kang S, Luo L, Shi Q, Ma J, Yin J, Song B, Hu D & Yang S, *Chem Central J*, **7** (2013) 64.
2 Bourbon P, Peng Q, Ferraudi G, Stauffacher C, Wiest O & Helquist P, *J Org Chem*, **77** (2012) 2756.
3 Ferris J P, Kuder J E & Catalano A W, *Science,* 166 (1969) 765.
4 Qiu Q, Shi W, Li Z, Zhang B, Pan M, Cui J, Dai Y, Huang W & Qian H, *J Med Chem*, 60 (2017) 2930.
5 Peng M, Shi L & Ke S, *Chem Central J,* 11 (2017) 109.
6 Ye Y H, Ma L, Dai Z C, Xiao Y, Zhang Y Y, Li D D, Wang J X & Zhu H L, *J Agric Food Chem,* 62 (2014) 4063.
7 Girgis A D, Hosni H M & Barsoum F F, *Bioorg Med Chem,* 14 (2006) 4466.
8 Kolb H & Burkart V, *Diabetes Care,* 22 (1999) B16.
9 Eugen J, Marian K, Milan M & Jerzy M, *J Coord Chem,* 40(3) (1996) 167.
10 Maiese K & Chong Z Z, *Trends PharmacolSci,* 24(5) (2003) 228.
11 Elliott R B, Pilcher C C, Fergusson D M & Stewart A W, *J Ped Endocrin Metabol,* 9 (1996) 501.
12 Yang Z, Guo L, Zhou C, Wang X, Yu M, Xul M & Yang K, *J Pestic Sci,* 45 (2020) 39.
13 Hamoud M M S, Pulya S, Osman N A, Bobde Y, Hassan A E A, Abdel-Fattah H A, Ghosh B & Ghanim A M, *New J Chem,* 44 (2020) 9571.
14 Taşkın Kafa A H, Tüzün G, Güney E, Aslan R, Sayin K, Tüzün B & Ataseven H, *Struc Chem*, 33 (2022) 1189.
15 Dennington R, Keith T A & Millam J M, *Gauss View, Version 6.1*, (Semichem Inc, Shawnee Mission, KS) 2016.
16 Frisch M J, Trucks G W, Schlegel H B, Scuseria G E, Robb M A, Cheeseman J R, Scalmani G, Barone V, Petersson G A, Nakatsuji H, Li X, Caricato M, Marenich A V, Bloino J, Janesko B G, Gomperts R, Mennucci B, Hratchian H P, Ortiz J V, Izmaylov A F, Sonnenberg J L, Williams-Young D, Ding F, Lipparini F, Egidi F, Goings J, Peng B, Petrone A, Henderson T, Ranasinghe D, Zakrzewski V G, Gao J, Rega N, Zheng G, Liang W, Hada M, Ehara M, Toyota K, Fukuda R, Hasegawa J, Ishida M, Nakajima T, Honda Y, Kitao O, Nakai H, Vreven T, Throssell K, Montgomery J A, Peralta J E, Ogliaro F, Bearpark M J, Heyd J J, Brothers E N, Kudin K N, Staroverov V N, Keith T A, Kobayashi R, Normand J, Raghavachari K, Rendell A P, Burant J C, Iyengar S S, Tomasi J, Cossi M, Millam J M, Klene M, Adamo C, Cammi R, J Ochterski W, Martin R L, Morokuma K, Farkas O, Foresman J B & Fox D J, *Gaussian 16, Revision B.01*, (Gaussian Inc., Wallingford CT) 2016.
17 Elmer P, *Chem Bio Draw Ultra Version*, (13.0.0.3015), 2012.
18 Eloff J N, *Planta Medica*, 64 (1998) 711.
19 Celik C, Tutar U, Karaman İ, Hepokur C & Ataş M, *Int J Pharmacol*, 12 (2016) 28.
20 Flemming H C, Wingender J, Szewzyk U, Steinberg P, Rice S A & Kjelleberg S, *Nature Rev Microbio,* 14 (2016) 563.
21 Dang T, Nizamov L S, Salikhov R Z, Sabirzyanova L R, Vorobey V V, Burganova T I, Shaidoullina M M, Batyeva E T, Cherkasov R A & Abdullin T I, *Bioorg Med Chem,* 27 (2019) 100.
22 Adamiec M, Adamus J, Ciebiada I, Denys A & Gebicki J, *Pharmacol Rep,* 58 (2006) 246.
23 Venkatasubramanian H, Sha S, Hemalatha S & Easwaramoorthy D, *Rasayan J Chem,* 12 (2019) 2005.
24 Shih Y H, Liu D, Chen Y C, Liao M H, Lee W R & Sheh S C, *Pharmaceutics,* 13 (2021) 819.
25 Kumar R N, Mallareddy G, Nagender P, Rao P S, Poornachandra Y, Ranjithreddy P & Narsaiah B, *Indian J Chem,* 55B (2016) 1361.